ACS OMEGA

http://pubs.acs.org/journal/acsodf

Article

Grafting Strategies of Oxidation-Prone Coiled-Coil Peptides for Protein Capture in Bioassays: Impact of Orientation and the Oxidation State

Médéric Dégardin, Jimmy Gaudreault, Romane Oliverio, Benjamin Serafin, Catherine Forest-Nault, Benoit Liberelle, and Gregory De Crescenzo*

Cite This: *ACS Omega* 2023, 8, 28301−28313

Read Online

ACCESS | Metrics & More | Article Recommendations | Supporting Information

ABSTRACT: Many biomedical and biosensing applications require functionalization of surfaces with proteins. To this end, the E/K coiled-coil peptide heterodimeric system has been shown to be advantageous. First, Kcoil peptides are covalently grafted onto a given surface. Ecoil-tagged proteins can then be non-covalently captured via a specific interaction with their Kcoil partners. Previously, oriented Kcoil grafting was achieved via thiol coupling, using a unique Kcoil with a terminal cysteine residue. However, cysteine-terminated Kcoil peptides are hard to produce, purify, and oxidize during storage. Indeed, they tend to homodimerize and form disulfide bonds via oxidation of their terminal thiol group, making it impossible to later graft them on thiol-reactive surfaces. Kcoil peptides also contain multiple free amine groups, available for covalent coupling through carbodiimide chemistry. Grafting Kcoil peptides on surfaces via amine coupling would thus guarantee their immobilization regardless of their terminal cysteine's oxidation state, at the expense of the control over their orientation. In this work, we compare Kcoil grafting strategies for the subsequent capture of Ecoil-tagged proteins, for applications such as surface plasmon resonance (SPR) biosensing and cell culture onto protein-decorated substrates. We compare the "classic" thiol coupling of cysteine-terminated Kcoil peptides to the amine coupling of (i) monomeric Kcoil and (ii) dimeric Kcoil−Kcoil linked by a disulfide bond. We have observed that SPR biosensing performances relying on captured Ecoil-tagged proteins were similar for amine-coupled dimeric Kcoil−Kcoil and thiol-coupled Kcoil peptides, at the expense of higher Ecoil-tagged protein consumption. For cell culture applications, Ecoil-tagged growth factors captured on amine-coupled monomeric Kcoil signaled through cell receptors similarly to those captured on thiol-coupled Kcoil peptides. Altogether, while oriented thiol coupling of cysteine-terminated Kcoil peptides remains the most reliable and versatile platform for Ecoil-tagged protein capture, amine coupling of Kcoil peptides, either monomeric or dimerized through a cysteine bond, can offer a good alternative when the challenges and costs associated with the production of monomeric cysteine-tagged Kcoil are too dissuasive for the application.

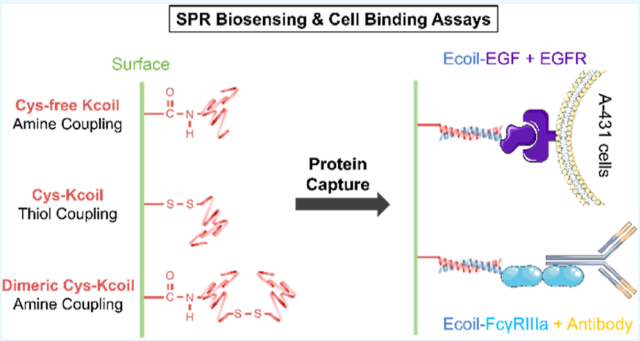

Downloaded via ECOLE POLYTECHNIQUE MONTREAL on September 13, 2023 at 19:11:39 (UTC).
See https://pubs.acs.org/sharingguidelines for options on how to legitimately share published articles.

1. INTRODUCTION

Surface functionalization with proteins is used for various biomedical and biosensing applications.[1] One key challenge is maintaining the bioactivity of immobilized proteins,[2,3] i.e., preserving the integrity and accessibility of their binding site. As such, several immobilization strategies have been developed for the decoration of biomaterials with proteins.[4] These include protein adsorption directly on the biomaterial surface,[5,6] covalent grafting of the proteins,[7−9] as well as the design of chimeric proteins harboring bioengineered tags to promote capture on surfaces decorated with the complementary tag binder.[10,11] For this strategy, many interacting pairs have been reported: biotin/(strept)avidin,[12,13] Fc domain/protein A or G,[14,15] heparin-binding domain/heparin,[16,17] SH3 domain/peptide binding partners,[18,19] and natural or *de novo* designed coiled-coil peptidic heteromers.[20,21]

Among coiled-coils, the bioinspired Ecoil $(EVSALEK)_5$ and Kcoil $(KVSALKE)_5$ peptide pair has been successfully used for the oriented capture of bioactive proteins[22] in surface plasmon resonance (SPR) biosensing,[23−25] enzyme-linked immunosorbent assays (ELISA),[26] recombinant protein purification,[27] as well as capture of proteins on cell culture compatible surfaces[28] and hydrogels.[29] More specifically, fusion proteins have been genetically modified to express an Ecoil tag, while

Received: March 31, 2023
Accepted: July 14, 2023
Published: July 28, 2023

© 2023 The Authors. Published by American Chemical Society

the complementary Kcoil partner was covalently grafted onto a surface. The expression of proteins tagged with the Ecoil peptide, rather than the Kcoil, is mainly guided by the better yields observed with the former peptide in mammalian expression platforms.[30] As a result, the Kcoil partner has been preferred as the capture ligand, and several grafting strategies have been explored using specific amino acids added to the terminal ends of the Kcoil peptides.

The most reported Kcoil grafting strategy is covalent coupling via thiol chemistry, through a cysteine engineered at the N- or C-terminus of each Kcoil peptide.[31] The major limitation of this approach resides in the fact that the Kcoil peptide homodimerizes in a parallel fashion due to hydrophobic interactions when at high concentrations,[32] such as during harvesting at the end of chemical peptide synthesis or bacterial production.[33] This homodimerization in turn leads to the rapid formation of a disulfide bond between two cysteine-tagged Kcoils. This rapid oxidation phenomenon complicates peptide grafting and introduces variability in the yield of the grafting process. Moreover, increasing the grafting yield using reducing agents is not practically feasible as we have shown that such reagents deactivate the functional groups of the linkers used for thiol chemistry.[34] Since the Cys-Kcoil peptide is difficult and costly to produce by chemical synthesis due to its length, and difficulty to recover from bacterial production, we here evaluate alternative coupling chemistry that would negate the inclusion of a cysteine altogether, and avoid the issues associated with the terminal thiol functional group.

Since the Kcoil peptide possesses several free amine groups throughout its primary structure (those being originally designed to control hetero- versus homodimerization), it could instead be grafted through carbodiimide chemistry.[35] This would allow Kcoil peptides to be grafted regardless of the presence of cysteine and/or its oxidation state, at the expense of controlled orientation.

In this work, three Kcoil peptide grafting strategies were studied. First, to investigate whether including a cysteine in Kcoil could be avoided, cysteine-free Kcoil peptides (Cys-free Kcoil) were grafted via amine coupling onto carboxylic acid-exposing surfaces.[36] Then, for comparison sake, monomeric cysteine-terminated Kcoil peptides (Cys-Kcoil) were grafted by thiol coupling, through their unique N-terminus cysteine, onto thiol-reactive surfaces.[37] Finally, to verify whether Cys-Kcoil oxidation level monitoring and control could be omitted, dimeric Kcoil−Kcoil peptides (resulting from the oxidation of Cys-Kcoil) were grafted onto surfaces by amine coupling. The last approach was tested as Kcoil homodimers are known to rearrange upon addition of Ecoil peptides to form E/K coiled-coil heterodimers.[32] These Kcoil grafting strategies were tested by SPR biosensing to evaluate the stability of the Kcoil interaction with the Ecoil peptide, and the repeatability of assays aiming to measure protein−protein interactions between immobilized Ecoil-tagged ligands and solution analytes. For the study of protein−protein interactions using coiled-coil ligand capture, both weak (IgG with Ecoil-FcγRIIIa, $K_D \approx 700$ nM) or strong (EGFR with Ecoil-EGF, $K_D \approx 10$ nM) model systems were analyzed. These biosensor-based evaluations were complemented by cell culture experiments aiming at evaluating the potential of each Kcoil grafting strategy for biomedical applications.

2. MATERIALS AND METHODS

2.1. Chemical Reagents and Biological Materials. Cysteine-terminated Kcoil [CGG-$(KVSALKE)_5$, Cys-Kcoil) and cysteine-free azidohomoalanine-terminated Kcoil (AhaGG-$(KVSALKE)_5$, Cys-free Kcoil)] peptides were synthesized at the University of Sherbrooke (QC, Canada) on a Symphony X solid-phase peptide synthesizer (Gyros Protein Technologies). Peptides were purified by preparative inverse-phase high-performance liquid chromatography and characterized by mass spectroscopy. The final purity was >99.9%. The Ecoil peptide [$(EVSALEK)_5$] was synthesized at the University of Colorado (CO, USA) on a CEM Liberty System microwave-assisted synthesizer (Matthews, NC), purified, and characterized as previously described.[38] The final purity was >95%. All peptides used in this study underwent N-terminal acetylation and C-terminal amidation. FcγRIIIa (V158 mutant) tagged with an Ecoil peptide and the wild-type monoclonal IgG *Trastuzumab* (TZM) were produced by transient transfection in CHO-3E7 cells and purified as shown in the work of Cambay et al.[23] Briefly, Ecoil-tagged FcγRIIIa was purified by ion metal affinity chromatography, and TZM was purified by protein A affinity chromatography. Both proteins were then further purified by size-exclusion chromatography to remove protein aggregates (final % of aggregates: <5%.[23]) EGF protein bearing a polyhistidine arm with an Ecoil tag at its end (Ecoil-EGF) was produced by transient transfection in HEK293-6E cells and purified by immobilized-ion affinity chromatography and size exclusion chromatography as shown in the work of Boucher et al.[30] The purified, aggregate-free protein was characterized by SDS-PAGE[30] and ELISA, R&D Systems #DY236) and stored at −80 °C until use. Recombinant human EGF (hEGF, #236-EG) and EGFR-Fc chimera (EGFR, #344-ER) proteins were purchased from R&D Systems. Mouse anti-phosphotyrosine primary antibody (PY99) was purchased from Santa Cruz Biotechnology (#sc-7020). Mouse anti-β-actin primary antibody was purchased from Sigma-Aldrich (#1978). HRP-conjugated anti-mouse IgG was purchased from Novus (#NB7561).

Mercaptopropionic acid (#M5801), 3-aminopropyltriethoxysilane (APTES, #440140), sodium orthovanadate (phosphatase inhibitor, #56508), guanidium hydrochloride (#G3272), ethanolamine hydrochloride (#E6133), 5,5′-dithio-bis-(2-nitrobenzoic acid) (DTNB, #22582), and Tween20 (#P1379) were purchased from Sigma-Aldrich. Succinimidyl 3-(2-pyridyldithio)propionate (SPDP, #21857) N-hydroxysuccinimide (NHS, #24500), 1-ethyl-3-(3-dimethylaminopropyl)-carbodiimide hydrochloride (EDC, #22980), and lysis buffer (M-PER Mammalian Protein Extraction Reagent, #78503) were purchased from Thermo Fisher Scientific. Ethylenediaminetetraacetic acid (EDTA, # 409930010) was purchased from Fisher Scientific. 2-(2-pyridinyldithio) ethanamine hydrochloride (PDEA, #BR100058) was purchased from Cytiva. L-Cysteine (#173601000) was purchased from Acros Organics.

The A-431 (ATCC #CRL-1555) cell line was purchased from Cedarlane. Dulbecco's Modified Eagle's Medium (DMEM, ATCC #30-2002) and penicillin−streptomycin (ATCC #30-2300) were purchased from Cedarlane. Gibco's heat-inactivated fetal bovine serum (FBS, #A3840301) was purchased from Thermo Fisher Scientific.

All aqueous solutions and buffers were prepared with ultrapure Milli-Q water (Millipore Gradient A10 purification

https://doi.org/10.1021/acsomega.3c02172
ACS Omega 2023, 8, 28301−28313

system) and were filtered with 0.22 μm polyethersulfone membranes before use. HBS-EP buffer was prepared by diluting 10× HBS-EP buffer (#BR100669) from Cytiva. Acetate, borate, and PBS buffers were prepared from sodium acetate (#S2889), sodium tetraborate (#229946), and saline phosphate (#P5368) powders purchased from Sigma-Aldrich.

2.2. Kcoil Peptide Grafting Strategies for Protein Capture in SPR Biosensing. All SPR experiments were performed on a Biacore T100 biosensor, which uses the geometry proposed by Kretschmann and Raether.[39,40] Gold CM5 sensor chips (Cytiva) bearing a layer of carboxymethylated dextran were used. The running buffer was HBS-EP. The experiments were conducted at 25 °C with a data collection rate of 10 Hz. Two 15 s pulses of 6 M guanidium-HCl were used to regenerate the Kcoil surfaces between cycles.

2.3. Kcoil Grafting via Amine Coupling. Covalent grafting of Kcoil through amine coupling was performed according to a previously published protocol.[36] The sensor chip surface was activated at 25 °C by injecting 0.4 M EDC and 0.1 M NHS mixed at a 1:1 (v/v) ratio for 7 min at 20 μL/min. Cysteine-free azidohomoalanine-terminated Kcoil (Cys-free Kcoil) was selected. Cys-free Kcoil was diluted in a 10 mM acetate buffer at pH 5.0 and was injected on the experimental surface at a concentration of 167 μg/mL through 15 s pulses at 20 μL/min until the required density was reached: 200 RU for the low-density surface and the highest possible (1000 RU) for the high-density surface. Then, the remaining active sites were blocked by injecting ethanolamine (1 M at pH 8.5) at 20 μL/min for 4 min. Before and after the surface preparation, the system was extensively primed with a running buffer (HBS-EP).

2.4. Kcoil Grafting via Thiol Coupling. Covalent grafting of Kcoil via thiol coupling was performed according to a previously published protocol.[37] The thiol coupling reagent PDEA was first immobilized on the sensor surface via amine coupling. The sensor chip was activated at 25 °C with NHS/EDC through a 4 min injection at 5 μL/min. Then, 1.8 mg of PDEA was dissolved in 150 μL of 50 mM borate (pH 8.5) and injected for 8 min at 5 μL/min. Ethanolamine (4 min, 5 μL/min) was then injected to deactivate the surface. Cys-Kcoil was diluted in 100 mM acetate (pH 4.5) to obtain a Kcoil concentration of 167 μg/mL. This solution was injected in 15 s pulses until the target density was reached: 15 RU for the low-density surface and the highest possible (2500 RU) for the high-density surface. Finally, a cysteine-NaCl solution made by diluting 3 mg of L-cysteine and 14 mg of NaCl in 500 μL of acetate (100 mM, pH 4.5) was injected at 5 μL/min for 4 min to deactivate the unreacted PDEA groups.

2.5. Kcoil Homodimerization and Grafting via Amine Coupling. Kcoil−Kcoil peptides (dimeric Cys-Kcoil) were naturally formed by the oxidation of cysteine residues at the end of Cys-Kcoil peptides. Cys-Kcoil peptides (1 mg/mL in Milli-Q water) were left at room temperature (RT) for 72 h. Before further use, the proportion of Cys-Kcoil peptides that remained monomeric was evaluated by measuring the quantity of free thiols with Ellman assays.[41] In brief, samples were diluted in PBS (100 mM, pH 7.4) supplemented with 1 mM EDTA, 720 μM DTNB and 0.025% v/v Tween20, in a clear 96-well microplate. After 1 min, the concentration of free thiols in the sample was measured by absorbance at 405 nm (with a correction at 630 nm) on a Victor V microplate reader from Perkin Elmer.

Next, amine covalent grafting of the dimeric Cys-Kcoil was performed in the same way as the grafting of Cys-free Kcoil (amine coupling). The low-density surface contained 350 RU of dimeric Kcoil, and the high-density surface contained 1500 RU.

2.6. SPR Experiments for Ecoil−Kcoil Interaction Measurements. Kcoil was grafted either through amine coupling or through thiol coupling (see above). To evaluate the dissociation rate of the Ecoil−Kcoil complex, six Ecoil concentrations (from 5 to 200 nM) were injected in duplicates. The injection time was 200 s, and the dissociation time was 700 s. The injection flow rate was set to 50 μL/min. A mock surface (for referencing purposes) was generated by activating/deactivating the surface with the same solutions (without any Kcoil injections). Blank injections were performed for double referencing purposes.[42]

2.7. Estimation of the Ecoil−Kcoil Complex Dissociation. Assuming a 1:1 interaction, the dissociation kinetics are described by the following equation

$$R(t) = R_{t_{off}} \exp(-k_{d,app}(t - t_{off})) \quad (1)$$

where $R(t)$ is the SPR response in time (in RU), t_{off} and $R_{t_{off}}$ are the time (in s) and SPR response at the start of the dissociation phase, and $k_{d,app}$ is the apparent estimated dissociation rate (in s^{-1}). This equation can be linearized

$$-\ln\left(\frac{R}{R_{t_{off}}}\right) = k_{d,app}(t - t_{off}) \quad (2)$$

As such, a graph of $-\ln\left(\frac{R}{R_{t_{off}}}\right)$ with respect to $(t - t_{off})$ shows all sensorgrams superimposed with a slope of $k_{d,app}$.

2.8. SPR Experiments to Measure the FcγRIIIa−IgG Interaction with the Ecoil−Kcoil System. Here, the Ecoil-tagged FcγRIIIa acts as the ligand: it is captured on the sensor surface through an Ecoil−Kcoil interaction. The IgG *Trastuzumab* (TZM) is then injected on the surface to act as the analyte: its binding to the ligand is measured via SPR. A SPR sensorgram is composed of a combination of an analyte injection phase (association phase) followed by a buffer injection phase (dissociation phase). Each cycle ended with a regeneration step to break the Ecoil−Kcoil bounds. New Ecoil-tagged FcγRIIIa was captured at the beginning of each cycle.

The Ecoil-tagged FcγRIIIa (0.25 μg/mL) was injected at 10 μL/min until the desired captured density was attained. To avoid mass transport limitations, a small quantity of FcγRIIIa was captured on the surface (approximately 20 RU). To this end, a short injection was performed to determine the rate of Ecoil-tagged FcγRIIIa capture on the Kcoil surfaces, and the Ecoil-tagged FcγRIIIa injection time used in the experiment was calculated by considering the capture rate to be constant. The association phase and dissociation phase times were set to 200 and 480 s, respectively, and the injection flow rate was 30 μL/min. The procedure was the same for all Kcoil surfaces.

2.9. Repeatability Assessment of the FcγRIIIa−IgG Interaction Measurements with the Ecoil−Kcoil System. To assess the repeatability of the SPR assay, two batches of 16 FcγRIIIa−IgG sensorgrams were recorded for each Kcoil surface. The FcγRIIIa injection time was calculated through an injection time test as mentioned above before each batch of experiments. A concentration of 270 nM of TZM was injected during the analyte injection phase. The FcγRIIIa capture level

https://doi.org/10.1021/acsomega.3c02172
ACS Omega 2023, 8, 28301−28313

as well as the FcγRIIIa−IgG sensorgrams were recorded (association and dissociation phase). To quantify the repeatability of the assay, we used the similarity score introduced by Karlsson et al.[43]

$$\text{similarity score} = \%\ \text{Pts in window} + \%\ \text{Pts out of window} \cdot \frac{SSQ_{\text{window-mean}}}{SSQ_{\text{points-mean}}} \quad (3)$$

The similarity score was calculated independently for the association and dissociation phases, as well as for each batch. A mean sensorgram was obtained for each batch by calculating the average SPR signal at every time step over all sensorgrams in a batch. The score tells us if a sensorgram is similar or not to the mean sensorgram. It consists of two terms. The first term is the proportion of data points comprised within a predefined window around the mean sensorgram. The second term penalizes sensorgrams for which data points outside of the similarity window are located far away from the limits of the window. Overall, a similarity score between 0% (dissimilar) and 100% (similar) is obtained for each sensorgram. The sensorgram-specific scores can be averaged to assess the repeatability of a particular grafting strategy.

2.10. SPR Experiments to Measure the EGF−EGFR Interaction with the Ecoil−Kcoil System. Here, Ecoil-EGF recombinant protein acted as the ligand, and the EGFR-Fc chimera (EGFR) acted as the analyte. Ecoil-EGF was injected at 10 μL/min until approximately 10 RU were captured on the sensor surface. An injection time test was previously performed to obtain the capture rate (RU/s). EGFR-Fc was injected during 480 s, followed by a 1250 s dissociation phase. Longer association and dissociation times were used due to the high avidity of the EGF−EGFR system. The injection flow rate was 30 μL/min. These parameters were the same for all Kcoil grafting methods. The Ecoil-EGF concentration was 0.1 μg/mL for the experiments with amine-coupled Kcoil and amine-coupled dimeric Kcoil and 0.05 μg/mL for thiol-coupled Kcoil.

2.11. Repeatability Assessment of the EGF−EGFR Interaction Measurements with the Ecoil−Kcoil System. The repeatability of the EGF−EGFR assay was evaluated similarly to that of the IgG−FcγRIIIa assay. Two batches of 16 sensorgrams were obtained, and the similarity scores were computed, as previously detailed. The EGFR concentration was 0.05 nM.

2.12. Cellular-Scale Study of Kcoil Peptide Grafting Strategies for Protein Capture. *2.12.1. Surface Preparation on Glass Slides.* Prior to functionalization, 1 cm × 1 cm glass slides (Erie Scientific Co.) were immersed for 24 h in KOH-saturated isopropanol for thorough cleaning and then extensively rinsed in Milli-Q water and air-dried. The slides were then functionalized to generate a thiol-reactive layer as previously described.[44] The slides were placed in an airtight container with 100 μL of APTES (four slides per container) and incubated overnight at RT for gas-phase deposit. They were then incubated for 2.5 h at 120 °C to covalently bind the APTES layer, then rinsed in ethanol and Milli-Q water (twice), and air-dried.

The surfaces were then covered for 1 h at RT with 150 μL of SPDP, 2 mM in 90% PBS/10% DMSO, then rinsed in PBS and Milli-Q water (twice), and air-dried.

2.12.2. Kcoil Grafting via Thiol Coupling. Glass surfaces covered with APTES and SPDP were covered with 100 μL of a 5 μM solution of the Cys-Kcoil peptide in PBS, for 2 h at RT, then rinsed in PBS and Milli-Q water, and air-dried. The remaining active pyridyldithiol groups of the SPDP layer were blocked by covering the slides with 150 μL of a 50 μM L-cysteine solution in a saline acetate buffer (100 mM, pH 4.5, supplemented with 0.5 mM NaCl) for 1 h at RT. The surfaces were then rinsed in PBS and Milli-Q water (twice), air-dried, and stored at 4 °C in an airtight container until use.

2.12.3. Kcoil Grafting via Amine Coupling. To generate an amine-reactive layer, the glass surfaces functionalized with APTES and SPDP were covered for 1 h at RT with 150 μL of mercaptopropionic acid, 1 mM in PBS, then rinsed in PBS and Milli-Q water (twice), and air-dried. They were then covered by 150 μL of 0.1 M NHS and 0.4 M EDC at a 1:1 ratio (10 min, RT), rinsed in Milli-Q water (three times), and air-dried. Finally, the surfaces were covered with 100 μL of a 5 μM solution of the Cys-free Kcoil peptide in PBS, for 2 h at RT, then rinsed in PBS and Milli-Q water (twice), and air-dried. Cys-free Kcoil-functionalized surfaces were then stored at 4 °C in an airtight container until use.

2.13. Cell Culture. A-431 cells were maintained at 37 °C in a humid incubator, in complete medium: DMEM supplemented with penicillin−streptomycin and 10% FBS. Cells were passaged when they reached 85−90% confluence. "Basal medium" refers to DMEM + penicillin−streptomycin (without FBS).

2.14. Phosphorylation Assays. At t = 0 h, the Kcoil-functionalized surfaces were sterilized in 70% ethanol and then rinsed in sterile Milli-Q water. The following steps were performed under aseptic conditions as described in a previous study.[28] The surfaces were covered by 100 μL Ecoil-EGF (0, 1, 10, or 100 nM) in PBS and incubated at 37 °C for 2 h. The liquid was then collected and analyzed by ELISA to assess the grafting density of Ecoil-EGF, and the surfaces were rinsed three times in PBS. Cells were then passaged and resuspended in the basal medium and seeded on the surfaces: 100,000 cells/surface, in 100 μL of the basal medium, and incubated at 37 °C, 5% CO_2 for 5 h. After 4 h and 55 min, surfaces previously incubated without Ecoil-EGF were covered for 5 min with 100 μL of hEGF (0, 0.5, or 1 nM) in the basal medium as a positive control for rapid EGF-induced tyrosine phosphorylation of EGF receptor (EGFR).[45] Of interest, we have previously shown that hEGF and Ecoil-EGF have similar bioactivity in solution—EC_{50} = 4 nM for EGFR phosphorylation.[3]

All surfaces were then rinsed three times in PBS supplemented with 1 mM sodium orthovanadate and then covered with 100 μL of lysis buffer supplemented with 0.1 mM sodium orthovanadate. After 5 min, the surfaces were scraped and the liquid was collected and centrifuged (10,000g, 20 min) to remove insoluble material. Supernatants (lysates) were then stored at −80 °C until further characterization by western blot.

2.15. Western Blot. A431 lysates were analyzed for phosphotyrosine levels by western blot, using the mouse p-Tyr primary antibody. Before the assay, the global protein concentration was measured using the Bradford reagent, and the same protein amount was loaded in each well for gel electrophoresis. Similar loading of the wells was also controlled by probing for β-actin. HRP-conjugated anti-mouse IgG was used as the secondary antibody. Images were taken using a Gel Doc XR + system (Bio-Rad) and analyzed using the Image Lab v5.2.1 software (Bio-Rad).

https://doi.org/10.1021/acsomega.3c02172
ACS Omega 2023, 8, 28301−28313

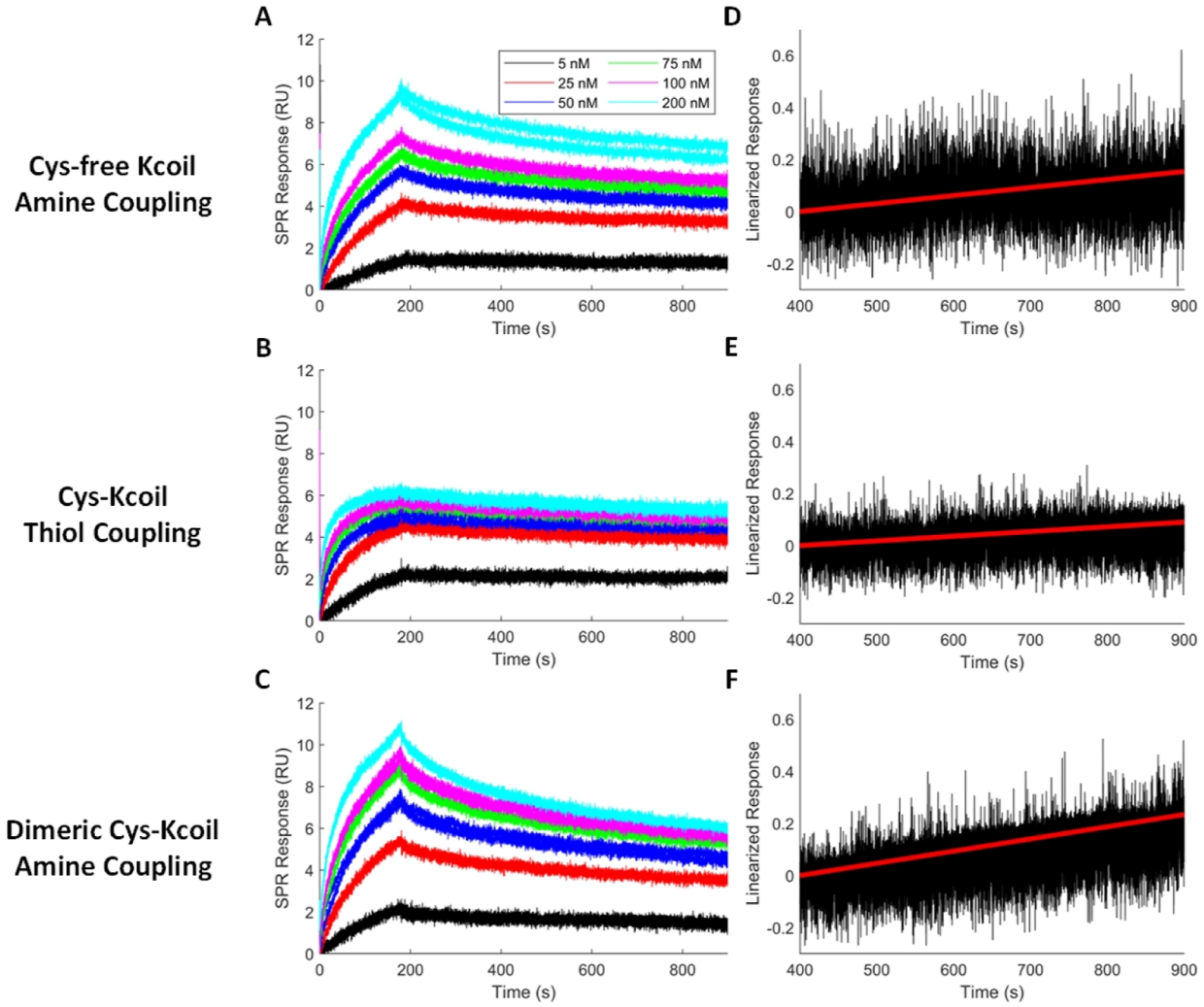

Figure 1. Ecoil binding to grafted Kcoil. SPR sensorgrams corresponding to Ecoil peptide injections over 200 RU of grafted Cys-free Kcoil by amine coupling (A), 15 RU of grafted Cys-Kcoil by thiol coupling (B), and 350 RU of grafted dimeric Cys-Kcoil by amine coupling (C). Sensorgrams were linearized and normalized (right panels, black). The slopes of the red fits estimate the apparent dissociation rate for the Cys-free Kcoil (D), the Cys-Kcoil (E), and the dimerized Cys-Kcoil (F) surfaces.

3. RESULTS

3.1. Kcoil Peptide Grafting Strategies for Protein Capture in SPR Biosensing. The performances of the three covalent grafting strategies were first evaluated by SPR biosensing.[39,40,42] The various Kcoil peptides were coupled to the carboxymethylated dextran coating of the SPR sensor chip. For each strategy, Ecoil as well as Ecoil-tagged proteins (Ecoil-FcγRIIIa and Ecoil-EGF) were then injected onto the Kcoil decorated sensor chips.[23,30] The ability of the captured Ecoil-tagged ligands to bind to their soluble complementary biological partners (the analytes in SPR terminology) was finally assessed for each Kcoil grafting strategy.

3.1.1. Ecoil Peptide Interaction with the Grafted Kcoil Peptide. First, the ability of i) amine-coupled Cys-free Kcoil, ii) thiol-coupled Cys-Kcoil, and iii) amine-coupled dimeric Cys-Kcoil to bind a single Ecoil peptide was evaluated. To that end, we grafted 200 RU of Cys-free Kcoil (amine coupling), 15 RU of Cys-Kcoil (thiol coupling), and 350 RU of dimeric Cys-Kcoil (amine coupling) peptides. These grafting levels were selected to avoid mass transport limitations. Amine-coupled Kcoil peptides were grafted to higher levels as the random grafting orientation reduced overall surface bioactivity (see below). Of interest, we performed Ellman assays[41] to determine that dimeric Cys-Kcoil peptides samples actually contained 74% (mass %) of dimers and 26% of monomers.

The dissociation rate constants for the Ecoil/Kcoil complexes were then determined, as they directly reflect the ability of the Kcoil surfaces to retain Ecoil-tagged proteins. The analysis was started after the initial 200 s of dissociation as the SPR sensorgrams showed a biphasic behavior with an initial rapid dissociation (Figure 1) followed by a slower dissociation, especially for the amine-coupled surfaces (Figure 1 A and C). The fastest Ecoil dissociation occurred with the amine coupling of dimeric Cys-Kcoil peptides (Table 1).

For proteins and peptides, the SPR signal is proportional to the mass accumulated at the sensor surface.[46] As Kcoil and

Table 1. Ecoil−Kcoil Interaction Characteristics as Measured via SPR for Different Kcoil Grafting Strategies

coupling	$k_{d,app}$ (10^{-4} s^{-1})	bioavailability
Cys-free Kcoil amine coupling	3.08 ± 0.02	5.00 ± 0.10%
Cys-Kcoil thiol coupling	1.80 ± 0.01	44.0 ± 3.00%
dimeric Cys-Kcoil amine coupling	4.68 ± 0.01	3.14 ± 0.06%

https://doi.org/10.1021/acsomega.3c02172
ACS Omega 2023, 8, 28301−28313

Ecoil peptides have approximately the same molecular weight (4 kDa), the SPR response reached for high concentrations of Ecoil peptides would approach the level of grafted Kcoil peptides, assuming all grafted Kcoil peptides were bioavailable. As such, we can estimate the overall bioavailability of a Kcoil-functionalized surface

$$\% \text{ bioavailability} = \frac{R_{\text{Analyte}}}{R_{\text{Ligand}}} \times 100 \quad (4)$$

Here, R_{Analyte} is the maximal response observed when injecting Ecoil peptides (the analyte) and R_{Ligand} is the grafting level of Kcoil peptides (the ligand); the SPR signal should be measured assuming that the surface is saturated with Ecoil peptides and all Kcoil peptides are bioavailable. The thiol-coupled Kcoil peptide surface was found to have the highest percentage of bioavailability. The dimeric Cys-Kcoil surface had a similar bioavailability and dissociation rate to the amine-coupled Cys-free Kcoil surface.

For amine-coupled Kcoil (monomeric and dimeric), the faster dissociation as well as the decreased bioavailability may be due to the inherent heterogeneity that results from amine coupling. Indeed, while thiol coupling can only occur through the N-terminal cysteine, amine coupling can take place on any of the 11 free amine groups present in the lysine side chains. Multiple amine groups allow for some Kcoil peptides to be grafted to the surface by more than one anchorage point. Overall, the amine coupling was most likely heterogeneous, with many of the coupled Kcoil peptides unable to form coiled-coil heterodimers. Kcoils grafted via a single amine may be affected differently in their interaction with the Ecoil, depending on the heptad in which the reacting lysine is located. Indeed, central heptads contribute more to the Ecoil/Kcoil interactions.[22,44] Also, multipoint grafting of a single Kcoil may occur, which further impedes its interaction with its Ecoil partner due to steric hindrance and a loss of conformational flexibility.

3.1.2. Grafted Kcoil Peptides as Capture Agents for IgG−FcγRIIIa Interaction Analysis. To assess the efficiency of the differently grafted Kcoils as capture molecules, we evaluated their ability to capture Ecoil-tagged FcγRIIIa (V158) for subsequent interaction with an IgG (*Trastuzumab*, TZM). The FcγRIIIa/IgG system was chosen due to its relatively weak binding affinity ($K_D \approx 700$ nM[23]), which would provide informative association and dissociation profiles (with appreciable curvature) depending on the preceding Kcoil grafting strategies.

Each experiment begins by capturing the Ecoil-FcγRIIIa (ligand). To avoid mass transport limitations, we aimed to capture a small quantity of ligands on the surface (20 RU). The required injection time was determined by extrapolating from a 25 s test injection (as seen in Table 2), assuming the capture rate (RU/s) was constant. Both methods based on amine chemistry had slower capture rates than the thiol-coupled method, most likely due to the random orientation of the Kcoils slowing down the formation of E/Kcoil heterodimers. Between amine coupling strategies, it is noteworthy that the dimeric Cys-Kcoil captures Ecoil-tagged FcγRIIIa more efficiently, which is consistent with the increased local concentration of Kcoil heptads.

Figure 2A−C shows the evolution of the ligand capture level, obtained with the required injection time reported in Table 2, for all Kcoil surfaces over two batches of 16 cycles. All three coupling strategies showed repeatable capture levels over a given batch of experiments. The FcγRIIIa capture level reached with amine-coupled Cys-free Kcoil was the furthest from the 20 RU target. Since the SPR response during the 25 s injection time test was smaller, the calculated capture rate (Table 2) is more uncertain.

Table 2. FcγRIIIa Injection Time Test

coupling	RU in 25 s	capture rate (RU/s)	required injection time for 20 RU (s)	FcγRIIIa consumed for 20 RU (ng)
Cys-free Kcoil amine coupling	1.4	0.06	357	14.9
Cys-Kcoil thiol coupling	14.2	0.57	35	1.5
dimeric Cys-Kcoil amine coupling	3.1	0.12	161	6.7

Figure 2D−F shows the corresponding IgG−FcγRIIIa interaction sensorgrams. To highlight the differences in kinetics, rather than the ligand capture level, all sensorgrams were normalized to 100% at the end of the analyte injection phase. Qualitatively, thiol coupling of Cys-Kcoil peptides and amine coupling of dimeric Cys-Kcoil peptides both led to repeatable responses, as the sensorgrams are well overlaid. On the other hand, amine-coupled Cys-free Kcoil displayed more variable kinetics over repeated injections, as seen by the poorly overlaid sensorgrams in Figure 2 D. Some cycles even showed negative values toward the end of the dissociation, indicative of ligand loss due to dissociation of the Kcoil−Ecoil complex.

To quantify this observation, we computed a similarity score.[43] For each batch of experiments, a mean sensorgram was calculated. Each sensorgram in the batch was then compared to the mean sensorgram to produce a similarity score (from 0% to 100%, with 100% being a perfect similarity score). The comparison window, that is the maximum deviation from the mean at which a sensorgram is considered similar, was varied from 0.1 to 1 RU. For each Kcoil peptide grafting method, the similarity scores of all 32 sensorgrams were averaged and are reported in Figure 3, and we defined the error bars by taking the standard deviation.

The amine coupling of Cys-free Kcoil had the worst similarity score. Overall, the sensorgrams obtained by grafting a dimeric Cys-Kcoil via amine coupling were similarly repeatable as those obtained by grafting Cys-Kcoil via thiol coupling.

3.1.3. Grafted Kcoil Peptides as Capture Molecules for EGF−EGFR Interaction Analysis. We also chose to study the impact of the initial Kcoil grafting strategy to capture ligands that bind to their analytes with high affinity, where only the association profile is relevant. To this end, we chose the epidermal growth factor (EGF)/EGF receptor (EGFR) system ($K_D \approx 10$ nM[47]). We captured Ecoil-EGF on Kcoil-functionalized surfaces functionalized using the three grafting strategies and then monitored the interactions with the soluble EGFR-Fc fusion proteins (EGFR). Table 3 indicates that the dimeric Kcoil had a nearly three times faster Ecoil-EGF capture rate compared to the monomeric Cys-free Kcoil. The capture rate of thiol-coupled Cys-Kcoil was even faster, despite the fact that a lower Ecoil-EGF concentration was used compared to the amine coupling-based strategies. These observations are in excellent agreement with those reported for Ecoil-FcγRIIIa (Table 2).

https://doi.org/10.1021/acsomega.3c02172
ACS Omega 2023, 8, 28301−28313

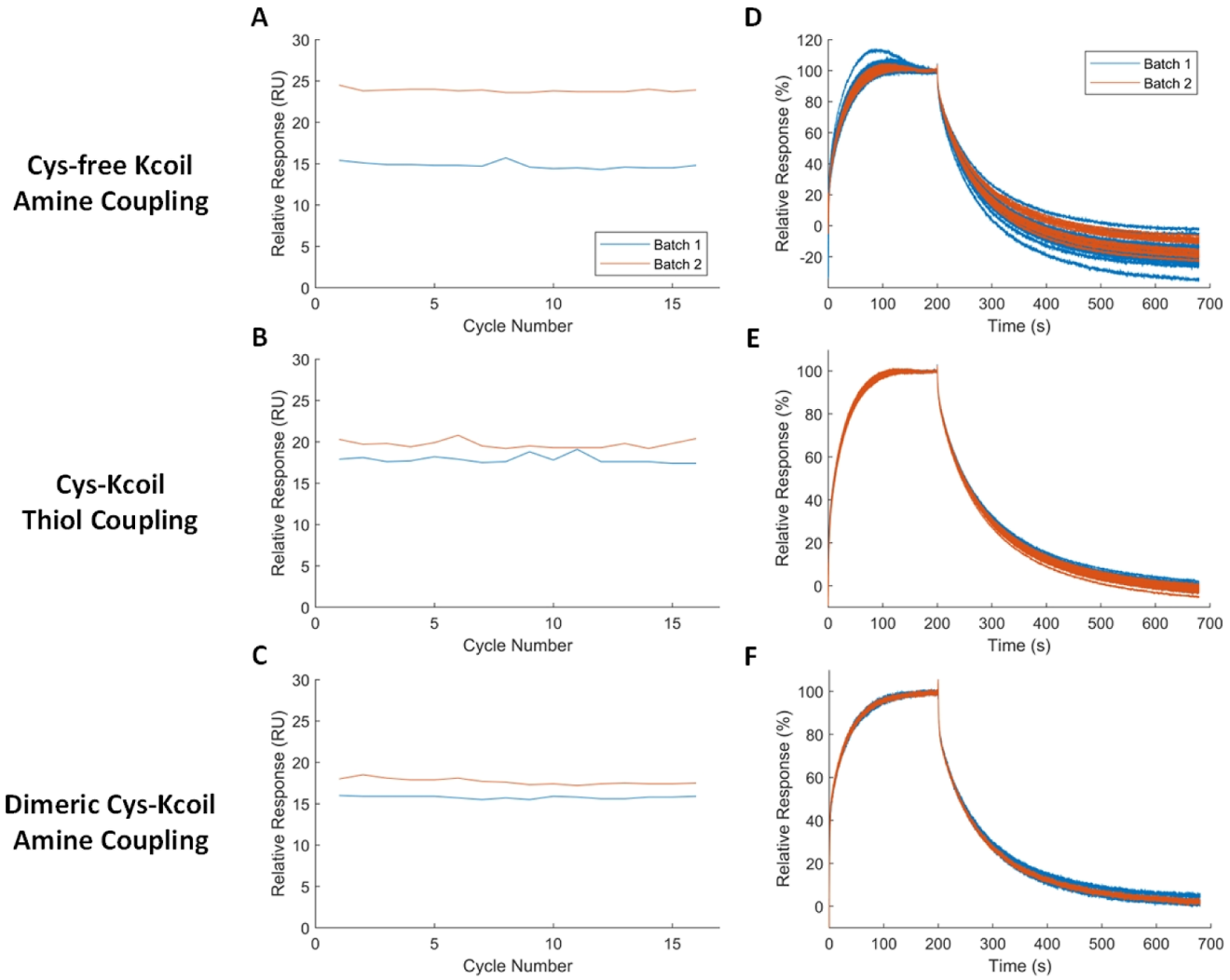

Figure 2. Repeatability of SPR biosensing experiments relying on coiled-coil-mediated capture of the ligand for different Kcoil grafting schemes. Ecoil-tagged ligand (FcγRIIIa V158) capture levels are evaluated with respect to the cycle number for two batches of experiments. The results are given for the amine-coupled Cys-free Kcoil (A), thiol-coupled Cys-Kcoil (B), and amine-coupled dimeric Cys-Kcoil (C). Overlaid sensorgrams of the interaction between TZM and FcγRIIIa$_{V158}$ are given for the same concentration of TZM injected in each cycle for amine-coupled Cys-free Kcoil (D), thiol-coupled Cys-Kcoil (E), and amine-coupled dimeric Cys-Kcoil (F).

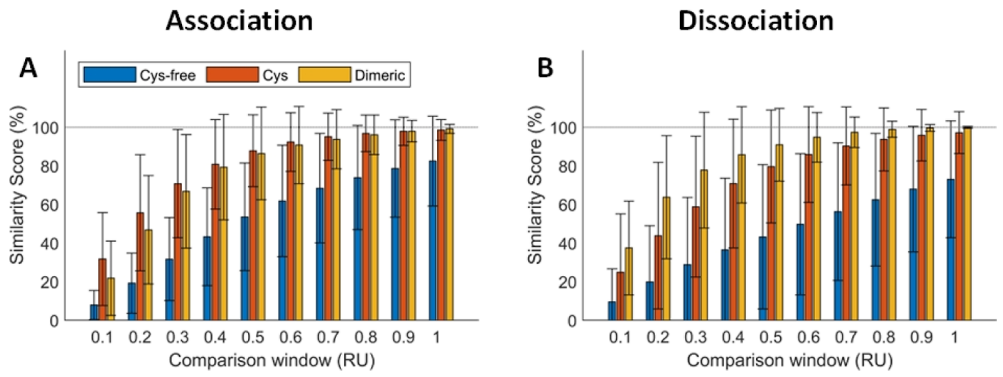

Figure 3. Similarity scores for the analysis of the interaction between TZM and Ecoil-FcγRIIIa (V158), where Ecoil-FcγRIIIa is captured by amine-coupled Cys-free Kcoil (blue bars), thiol-coupled Cys-Kcoil (orange bars), or amine-coupled dimeric Cys-Kcoil (yellow bars). The similarity scores were calculated independently both for the analyte injection phase (A) and the dissociation phase (B). A mean sensorgram was obtained for each of the two 16-sensorgram batches of experiments. All 16 sensorgrams within a batch were then compared to the mean sensorgram. Results show the average similarity score for both batches of all grafting methods, with a comparison window varying from 0.1 to 10 RU. The results obtained for each batch are shown in Figure S1.

https://doi.org/10.1021/acsomega.3c02172
ACS Omega 2023, 8, 28301−28313

Table 3. Ecoil-EGF Injection Time Test

coupling	Ecoil-EGF concentration (μg/mL)	RU in 25 s	capture rate (RU/s)	required injection time for 10 RU (s)	EGF consumed for 10 RU (ng)
Cys-free Kcoil amine coupling	0.1	8	0.32	32	0.5
Cys-Kcoil thiol coupling	0.05	33	1.32	8	0.1
dimeric Cys-Kcoil amine coupling	0.1	22	0.88	12	0.2

Figure 4A−C shows the capture level of Ecoil-EGF across two 16-cycle batches of experiments for each Kcoil peptides grafting strategy. Capture levels were repeatable within a batch, for all strategies. Thiol coupling had higher capture levels (approximately 15 RU instead of 10 RU). Ecoil-EGF injection time for this condition was 12 s, rather than 8 s as reported in Table 3, to accommodate the minimum injection volume of the biosensor.

Figure 4D−F shows the normalized sensorgrams for the corresponding EGF−EGFR interactions. Replicate sensorgrams were overlaid for all Kcoil peptides couplings. This system diverges from the results of the IgG−FcγRIIIa system, where the amine-coupled Cys-free Kcoil surface had several outlier sensorgrams. Figure 5 shows that all three strategies had comparable similarity scores, even for different comparison windows. This may result from the high stability of the EGF interaction with dimeric EGFR-Fc, leading to rebinding of EGFR-Fc to a nearby Ecoil-EGF, in turn obliterating the impact of the Kcoil coupling strategy.

Amine-coupled dimeric Cys-Kcoil thus appears to be a valid alternative grafting scheme to the "classical" thiol coupling approach as it showed similar repeatability in measured kinetics both with a weak (FcγRIIIa) and a strong (EGFR) system. Dimeric Cys-Kcoil is an unavoidable by-product of Cys-Kcoil synthesis, and using it in SPR experiments via amine coupling is a way to salvage an otherwise unusable oxidized stock. However, the immobilization rate associated with their use as capture agents was slower, in turn increasing the consumption of Ecoil-tagged proteins for biosensing experiments. Hence, it should be considered as a valid option when the Ecoil-tagged protein is not expensive.

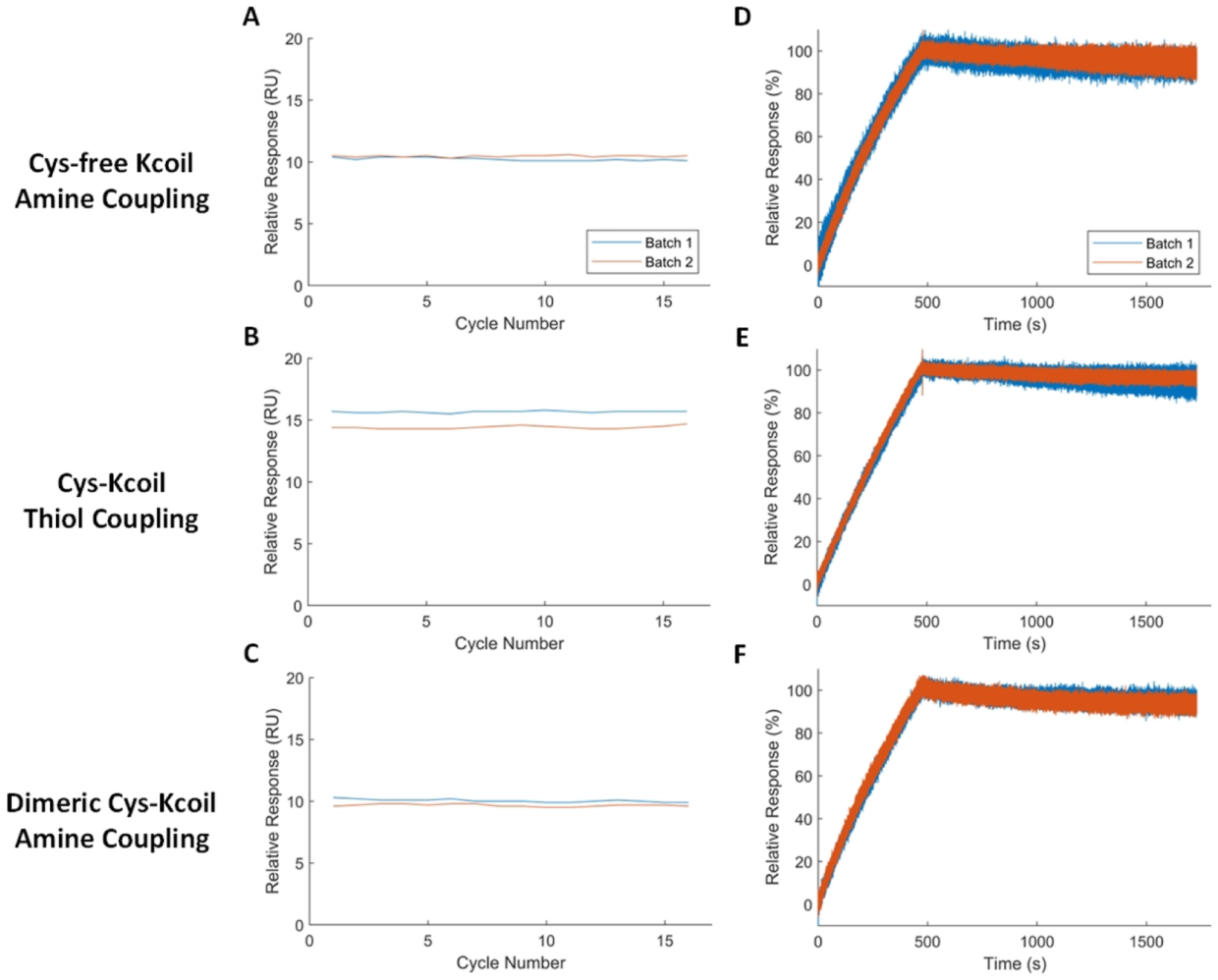

Figure 4. Repeatability of the Ecoil−Kcoil system for different Kcoil grafting strategies. Ligand (EGF) capture levels are evaluated with respect to the cycle number for two batches of experiments. The results are given for the amine-coupled Cys-free Kcoil (A), thiol-coupled Cys-Kcoil (B), and amine-coupled dimeric Cys-Kcoil (C). Overlaid sensorgrams of the interaction between EGFR and EGF are given for the same concentration of EGFR injected in each cycle for amine-coupled Cys-free Kcoil (D), thiol-coupled Cys-Kcoil (E), and amine-coupled dimeric Cys-Kcoil (F).

https://doi.org/10.1021/acsomega.3c02172
ACS Omega 2023, 8, 28301−28313

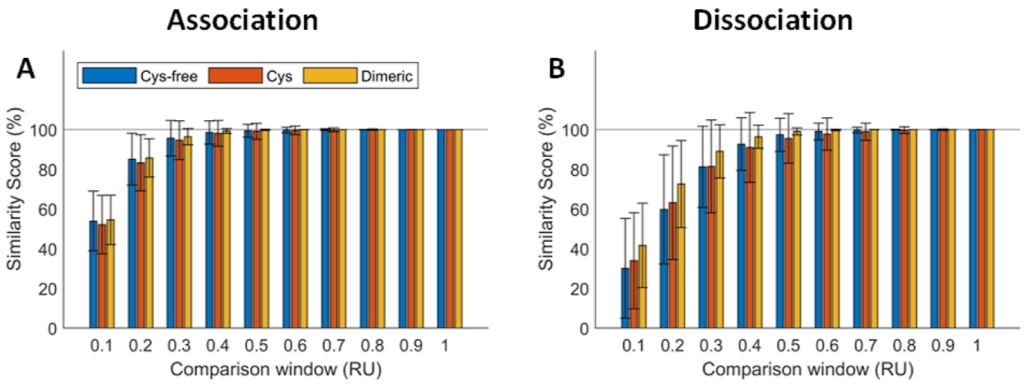

Figure 5. Similarity scores for the analysis of the interaction between EGFR-Fc and Ecoil-EGF, where Ecoil-EGF is captured by amine-coupled Cys-free Kcoil (blue bars), thiol-coupled Cys-Kcoil (orange bars), or amine-coupled dimeric Cys-Kcoil (yellow bars). The similarity scores were calculated independently both for the analyte injection phase (A) and the dissociation phase (B). A mean sensorgram was obtained for each of the two 16-sensorgram batches of the experiment. All 16 sensorgrams within a batch were then compared to the mean sensorgram. Results show the average similarity score for both batches of all grafting methods, with the comparison window varying from 0.1 to 1 RU. The results obtained for each batch are shown in Figure S2.

4. CELLULAR-SCALE STUDY OF KCOIL PEPTIDE GRAFTING STRATEGIES FOR PROTEIN CAPTURE

Another goal of this study was to assess the impact of Kcoil peptide grafting strategies for protein capture at the cellular scale. The rationale behind this approach was to establish whether, for surface biofunctionalization purposes, the oriented grafting of Kcoil provides an advantage in terms of the final biological outcome. Indeed, while SPR and related biosensing assays provide real-time, kinetic insight into the observed systems, the phenomena observed at the cellular level are more complex with potential diffusion limitations and characterized by longer timescales.

The cellular assays were performed by grafting Kcoil peptides on functionalized glass slides[44] and capturing Ecoil-EGF proteins.[28] A-431 cells were subsequently inoculated and incubated on the Ecoil-EGF-functionalized glass surfaces. At the cellular scale, EGF binding to cell surface EGFR induces transient EGFR phosphorylation in A431 cells, followed by the internalization and degradation of the EGF/EGFR complex.[45] We previously demonstrated that in solution, Ecoil-tagged EGF has a similar bioactivity to wild-type EGF (EC_{50} = 4 nM for EGFR phosphorylation[30]). Thus, the bioavailability of the Ecoil-EGF proteins attached to the glass surfaces was here assessed by phosphorylation assays of EGFR depending on the initial Kcoil peptide grafting strategy.

In a previous study by Boucher et al.,[28] we demonstrated that Ecoil-EGF captured via coiled-coil interactions on a thiol-coupled Kcoil surface retained its bioactivity, and induced sustained EGFR phosphorylation by preventing EGF internalization. Here, we focus on the influence of the Kcoil coupling strategy on the bioactivity of Ecoil-EGF captured via coiled-coil interactions. Besides the thiol coupling strategy, we studied the amine coupling of Cys-free Kcoil. Ecoil-EGF was incubated on amine- and thiol-coupled Kcoil surfaces, which were then rinsed to remove unbound Ecoil-EGF. Next, A431 cells were seeded and incubated for 5 h. Cell lysates were then collected and probed for EGFR phosphorylation levels by Western blot (Figure 6).

The capture level of Ecoil-EGF after the initial 2 h incubation was estimated by probing the Ecoil-EGF solution by ELISA, before and after the incubation (Table 4). When incubating the surfaces with low concentrations of Ecoil-EGF

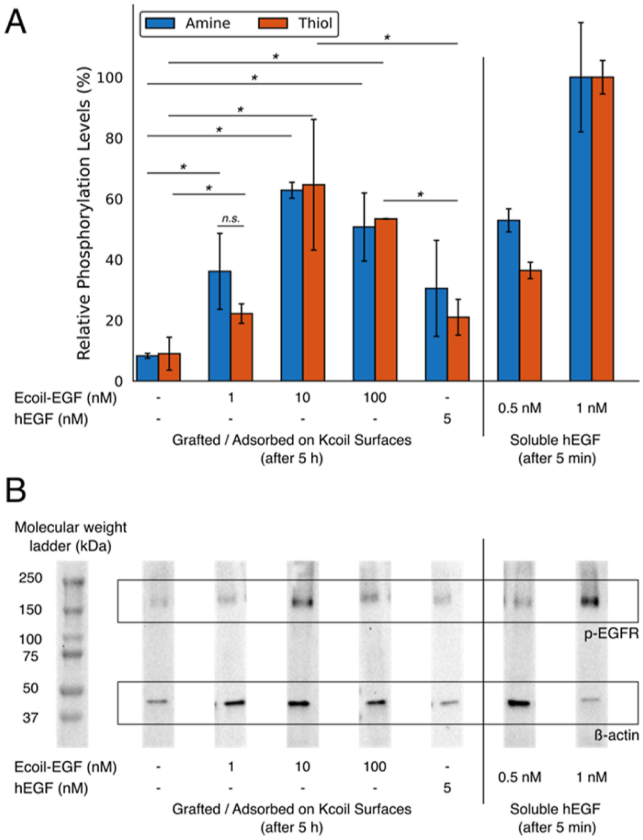

Figure 6. (A) Bioactivity of grafted Ecoil-EGF based on the coupling strategy used for the functionalization of the surfaces with Kcoil. Bioactivity is measured by Western blot in terms of relative EGFR phosphorylation levels. The signal is normalized to the signal obtained for the transient phosphorylation (after 5 min of exposure) of EGFR by 1 nM hEGF in solution and compared to the signal obtained when hEGF is non-specifically adsorbed on the surfaces. Values are mean ± standard deviation (n = 3). *p < 0.05 indicates statistically significant differences in bilateral t-test pairwise comparisons. (B) Representative western blot showing protein levels of phosphorylated EGFR (p-EGFR, ∼180 kDa) and β-actin (∼42 kDa) when surfaces are functionalized using amine coupling.

(1 or 10 nM), both amine and thiol coupling strategies allowed for similar levels of Ecoil-EGF capture (>98% of the incubated

https://doi.org/10.1021/acsomega.3c02172
ACS Omega 2023, 8, 28301−28313

Table 4. Density of Ecoil-EGF and hEGF Captured via Coiled-Coil Interaction or Non-specific Adsorption on the Glass Slides, after the Initial 2 h of Incubation[a]

concentration of stock solutions	Ecoil-EGF			hEGF
captured after 2 h	1 nM	10 nM	100 nM	5 nM
on amine surface (pmol/cm^2)	0.100 ± 0.001	1.00 ± 0.02	6.00 ± 1.00	0.50 ± 0.01
on thiol surface (pmol/cm^2)	0.100 ± 0.001	1.00 ± 0.02	9.50 ± 0.10	0.50 ± 0.01

[a]Values (mean ± standard deviation, $n = 3$) are measured by ELISA by comparing the concentration in EGF moieties before and after incubation.

amount). When increasing the concentration of Ecoil-EGF to 100 nM, thiol-coupled Kcoil captured almost all the incubated Ecoil-EGF (>95%). For amine-coupled Kcoil, this amount dropped to ≈60% of the incubated amount. This difference ($p < 0.01$, bilateral t-test, $n = 3$) indicates that the oriented, N-terminal thiol coupling of Cys-Kcoil proves more efficient for the capture of Ecoil-tagged molecules than the amine coupling.

For all concentrations of Ecoil-EGF, western blot probing of A431 cell lysates evidenced similar levels of EGFR phosphorylation, regardless of the Kcoil grafting strategy (Figure 6). Five hours after the seeding of the cells on the Ecoil-EGF-functionalized glass surfaces, sustained phosphorylation is observed. The intensity of this sustained phosphorylation reaches 50−60% of the levels obtained when directly incubating the cells with 1 nM hEGF in solution for 5 min (transient phosphorylation). For both grafting conditions, a 10-fold increase (1 to 10 nM, Table 4) in the amount of grafted Ecoil-EGF leads to a 2-fold increase in the phosphorylation level. Furthermore, increasing the Ecoil-EGF amount to 100 nM does not lead to increased phosphorylation, indicating that a threshold is reached. Interestingly, we show that Ecoil-EGF captured through coiled-coil interactions is more efficient than non-specifically adsorbed hEGF, especially when using the thiol coupling strategy.

Altogether, these results demonstrate that despite the thiol coupling strategy allowing for more efficient capture of Ecoil-EGF above a certain concentration threshold (Table 4), this increase has no significant effect on EGF signaling (Figure 6). This result is in line with what was previously observed by our research group,[48] where Murschel et al. reported a consistent biological outcome when capturing Ecoil-tagged growth factors by oriented adsorption. In all respects, at the cellular scale, there is thus no incentive to favor one grafting strategy over the other in terms of experimental efficiency.

5. DISCUSSION

Our research group uses the E/K coil system in a great variety of applications by grafting Cys-Kcoil to various surfaces through thiol chemistry. Examples include SPR assays (for the interaction of antibodies[23,49,50] and growth factors[37] with their respective receptor) as well as other bioassays such as ELISA[26] for biomaterial functionalization[28,31,51] and controlled gene delivery.[52] Cys-Kcoil production and storage are difficult as this peptide is prone to oxidation, leading to dimeric Kcoil−Kcoil by-products. Cys-Kcoil can be produced in two ways. The first way is by chemical peptide synthesis. However, Kcoil is costly to produce in this fashion because of its length (35 amino acids for Kcoil and 38 for Cys-Kcoil) and its propensity to aggregate during synthesis. A monomeric, little-oxidized Cys-Kcoil is obtained, but it will undergo oxidation in time. The second way is by cell culture. Since short peptides such as Kcoil (including Cys-Kcoil) do not require post-translational modifications, bacteria are an appropriate expression system. In that endeavor, our research group has previously shown that fusing the Cys-Kcoil to a subsequently cleaved chaperone protein improved its solubility and increased its production levels in bacteria.[33] However, we found that a significant amount of thus-produced Cys-Kcoil had undergone dimerization through oxidation during the purification process, rendering them unsuitable for thiol chemistry.[33]

Reducing the disulfide bond could theoretically reactivate the Cys-Kcoil, but we observed that reducing agents deactivated the functional groups of the linkers typically used to perform the thiol chemistry.[34] Hence, reversing the oxidation to subsequently perform the grafting is not practically feasible. Therefore, producing a Kcoil that is devoid of any cysteine residue (Cys-free Kcoil) would be preferable as there would be no need to monitor/control the oxidation level, rendering large-scale production in a bioreactor possible.

Since the Kcoil peptide contains multiple lysine residues, we thus studied the impact of grafting the Kcoil through amine coupling instead of thiol coupling via SPR. We found that thiol coupling of Cys-Kcoil produced surfaces with a greater capacity to interact with complementary single Ecoil peptides and form E/K coiled-coil heterodimers, likely due to grafting heterogeneity and steric hindrance in the amine coupling scheme (Figure 1; Table 1). Then, Ecoil-tagged proteins were captured onto both surfaces, and their interactions with complementary analytes were assessed. We found that Ecoil-tagged proteins bound the thiol-coupled Kcoil substantially faster than the amine-coupled Kcoil, implying that a greater amount of Ecoil-tagged protein must be used with Cys-free Kcoil, which renders assays more costly, a major caveat when the Ecoil-tagged protein is expensive (Tables 2 and 3). Nevertheless, when the captured Ecoil-tagged protein had a high affinity for its analyte (such as in the case of the EGFR/EGF-Ecoil biological system), no difference was observed between the ligand-analyte sensorgrams recorded with the two Kcoil capture strategies (Figures 4 and 5). However, when the affinity of the system was weak (IgG/Ecoil-FcγRIIIa), the amine-coupled surface showed poor repeatability (Figures 2 and 3). We then compared the two strategies at the cellular scale with an in vitro phosphorylation assay. Of salient interest, here we found similar performance for both grafting strategies (Figure 6). Overall, our findings indicate that SPR exhibits a certain sensitivity to the grafting strategy, pointing to the fact that Cys-Kcoil remains preferable for SPR studies, while assays at a larger scale are not impacted by the Kcoil coupling.

In parallel to these experiments, we also tested an SPR surface onto which oxidized dimeric Kcoil-Cys-Cys-Kcoil was grafted with amine chemistry, as a way to potentially salvage Cys-Kcoil lots that had undesirably oxidized. While Ecoil-tagged protein capture was also slow on such a surface, it interestingly exhibited similar repeatability as that of the thiol-coupled surface in all SPR studies performed (Figures 2−5). Hence, if a Cys-Kcoil lot has undergone oxidation, it remains usable, only with a different grafting strategy. This, however,

https://doi.org/10.1021/acsomega.3c02172
ACS Omega 2023, 8, 28301−28313

only makes sense when the Ecoil-tagged ligand is not expensive, as the amine-coupled dimeric Kcoil surface captured the ligand 2 to 5 times slower than the thiol-coupled Kcoil surface, leading to a greater Ecoil-tagged protein consumption (Tables 2 and 3).

As SPR only requires small amounts of Kcoil (less than a microgram per functionalized SPR surface, which can be used for up to 1000 cycles[23]), we still recommend using thiol-coupled Cys-Kcoil for SPR assays, even with increased Cys-Kcoil production costs. Our novel finding resides in the results of our cellular studies. Indeed, it appears that Cys-free amine-coupled Kcoil is an appropriate alternative to thiol-coupled Cys-Kcoil for such an application. This opens the door to diminishing production costs related to Kcoil peptides. This is of even greater interest as studies at this scale often require far greater amounts of Kcoil peptides to be conducted. For example, the functionalization of all surfaces used for the cell studies in this manuscript required approximately 60 μg of Kcoil peptides, affinity-based hydrogels previously reported by our group required up to 10 μg of Kcoil per single-use gel,[29] and auto-assembled gels reported by others necessitate up to 500 μg of Kcoil per gel [.[53]

Overall, we conclude that a randomly oriented, amine-mediated grafting of Kcoil peptides can be an alternative to the traditionally oriented thiol-mediated grafting in studies involving large amounts of Kcoil to decorate surfaces and gels. This can circumvent the issue of thiol oxidation observed with cysteine-terminated Kcoil peptides, allowing for a more repeatable and controlled grafting procedure as the oxidation level is variable in time and impacts thiol coupling. Moreover, the use of amine coupling approaches would ease large-scale biomanufacture of Kcoil peptides as there would be no need to prevent or control oxidation.

■ ASSOCIATED CONTENT

Supporting Information

The Supporting Information is available free of charge at https://pubs.acs.org/doi/10.1021/acsomega.3c02172.

Similarity scores for TZM/FcγRIIIa, and similarity scores for EGFR-Fc/EGF (PDF)

■ AUTHOR INFORMATION

Corresponding Author

Gregory De Crescenzo − *Department of Chemical Engineering, Polytechnique Montréal, Montréal H3T 1J4 Québec, Canada;* orcid.org/0000-0002-6280-1570; Email: gregory.decrescenzo@polymtl.ca

Authors

Médéric Dégardin − *Department of Chemical Engineering, Polytechnique Montréal, Montréal H3T 1J4 Québec, Canada*

Jimmy Gaudreault − *Department of Chemical Engineering, Polytechnique Montréal, Montréal H3T 1J4 Québec, Canada*

Romane Oliverio − *Department of Chemical Engineering, Polytechnique Montréal, Montréal H3T 1J4 Québec, Canada*

Benjamin Serafin − *Department of Chemical Engineering, Polytechnique Montréal, Montréal H3T 1J4 Québec, Canada*

Catherine Forest-Nault − *Department of Chemical Engineering, Polytechnique Montréal, Montréal H3T 1J4 Québec, Canada*

Benoit Liberelle − *Department of Chemical Engineering, Polytechnique Montréal, Montréal H3T 1J4 Québec, Canada*

Complete contact information is available at: https://pubs.acs.org/10.1021/acsomega.3c02172

Author Contributions

All authors equally contributed to this manuscript.

Notes

The authors declare no competing financial interest.

■ ACKNOWLEDGMENTS

This work was supported by the Natural Sciences and Engineering Research Council of Canada (stipends allocated to Médéric Dégardin, Jimmy Gaudreault, Romane Oliverio, Benjamin Serafin, and Catherine Forest-Nault via the NSERC-CREATE PrEEmiuM program) and by the TransMedTech Institute (NanoBio Technology Platform) and its main funding partner, the Canada First Research Excellence Fund. Parts of the figures were drawn using pictures from Servier Medical Art (smart.servier.com). Servier Medical Art by Servier is licensed under a Creative Commons Attribution 3.0 Unported License (http://creativecommons.org/licenses/by/3.0/). The authors would also like to thank Seyed Farzad Baniahmad (National Research Council of Canada) for his assistance regarding western blot procedures.

■ REFERENCES

(1) Tutar, R.; Motealleh, A.; Khademhosseini, A.; Kehr, N. S. Functional Nanomaterials on 2D Surfaces and in 3D Nanocomposite Hydrogels for Biomedical Applications. *Adv. Funct. Mater.* **2019**, *29*, 1904344.

(2) Wiseman, M. E.; Frank, C. W. Antibody adsorption and orientation on hydrophobic surfaces. *Langmuir* **2012**, *28*, 1765−1774.

(3) Secundo, F. Conformational changes of enzymes upon immobilisation. *Chem. Soc. Rev.* **2013**, *42*, 6250−6261.

(4) Rusmini, F.; Zhong, Z.; Feijen, J. Protein immobilization strategies for protein biochips. *Biomacromolecules* **2007**, *8*, 1775−1789.

(5) Wahlgren, M.; Arnebrant, T. Protein adsorption to solid surfaces. *Trends Biotechnol.* **1991**, *9*, 201−208.

(6) Zheng, K.; Kapp, M.; Boccaccini, A. R. Protein interactions with bioactive glass surfaces: A review. *Appl. Mater. Today* **2019**, *15*, 350−371.

(7) Fischer, M. J. Amine coupling through EDC/NHS: a practical approach. *Methods Mol. Biol.* **2010**, *627*, 55−73.

(8) Houseman, B. T.; Gawalt, E. S.; Mrksich, M. Maleimide-Functionalized Self-Assembled Monolayers for the Preparation of Peptide and Carbohydrate Biochips. *Langmuir* **2002**, *19*, 1522−1531.

(9) Coad, B. R.; Jasieniak, M.; Griesser, S. S.; Griesser, H. J. Controlled covalent surface immobilisation of proteins and peptides using plasma methods. *Surf. Coat. Technol.* **2013**, *233*, 169−177.

(10) You, C.; Bhagawati, M.; Brecht, A.; Piehler, J. Affinity capturing for targeting proteins into micro and nanostructures. *Anal. Bioanal. Chem.* **2009**, *393*, 1563−1570.

(11) Rao, S. V.; Anderson, K. W.; Bachas, L. G. Oriented immobilization of proteins. *Mikrochim. Acta* **1998**, *128*, 127−143.

(12) Hutsell, S. Q.; Kimple, R. J.; Siderovski, D. P.; Willard, F. S.; Kimple, A. J. High-affinity immobilization of proteins using biotin- and GST-based coupling strategies. *Methods Mol. Biol.* **2010**, *627*, 75−90.

(13) Wu, C. C.; Chiang, Y. H.; Chiang, H. Y. A Label-Free Electrochemical Impedimetric Immunosensor with Biotinylated-Antibody for SARS-CoV-2 Nucleoprotein Detection in Saliva. *Biosensors* **2022**, *12*, 265.

(14) Ingavle, G. C.; et al. Affinity binding of antibodies to supermacroporous cryogel adsorbents with immobilized protein A for removal of anthrax toxin protective antigen. *Biomaterials* **2015**, *50*, 140−153.

(15) Wong, W. C.; et al. Photonic Crystal Fiber Surface Plasmon Resonance Biosensor Based on Protein G Immobilization. *IEEE J. Sel. Top. Quantum Electron.* **2013**, *19*, 4602107.
(16) Lee, J. Y.; et al. Characterization of the surface immobilized synthetic heparin binding domain derived from human fibroblast growth factor-2 and its effect on osteoblast differentiation. *J. Biomed. Mater. Res. A* **2007**, *83*, 970−979.
(17) Linhardt, R.; Murugesan, S.; Xie, J. Immobilization of heparin: approaches and applications. *Curr. Top. Med. Chem.* **2008**, *8*, 80−100.
(18) Vulic, K.; Shoichet, M. S. Tunable growth factor delivery from injectable hydrogels for tissue engineering. *J. Am. Chem. Soc.* **2012**, *134*, 882−885.
(19) Silverman, B. R.; Champion, J. A. Presentation of fibronectin fragments using affinity protein interactions for enhanced retention and function. *Acta Biomater.* **2014**, *10*, 4956−4960.
(20) Utterstrom, J.; Naeimipour, S.; Selegard, R.; Aili, D. Coiled coil-based therapeutics and drug delivery systems. *Adv. Drug Delivery Rev.* **2021**, *170*, 26−43. Available:. https://www.ncbi.nlm.nih.gov/pubmed/33378707
(21) Jorgensen, M. D.; Chmielewski, J. Recent advances in coiled-coil peptide materials and their biomedical applications. *Chem. Commun.* **2022**, *58*, 11625−11636.
(22) De Crescenzo, G.; Litowski, J. R.; Hodges, R. S.; O'Connor-McCourt, M. D. Real-time monitoring of the interactions of two-stranded de novo designed coiled-coils: effect of chain length on the kinetic and thermodynamic constants of binding. *Biochemistry* **2003**, *42*, 1754−1763.
(23) Cambay, F.; et al. Impact of IgG1 N-glycosylation on their interaction with Fc gamma receptors. *Curr. Res. Immunol.* **2020**, *1*, 23−37.
(24) Forest-Nault, C.; et al. Impact of the temperature on the interactions between common variants of the SARS-CoV-2 receptor binding domain and the human ACE2. *Sci. Rep.* **2022**, *12*, 11520.
(25) Cachia, P. J.; Kao, D. J.; Hodges, R. S. Synthetic peptide vaccine development: measurement of polyclonal antibody affinity and cross-reactivity using a new peptide capture and release system for surface plasmon resonance spectroscopy. *J. Mol. Recognit.* **2004**, *17*, 540−557.
(26) Liberelle, B.; Bartholin, L.; Boucher, C.; Murschel, F.; Jolicoeur, M.; Durocher, Y.; Merzouki, A.; De Crescenzo, G. New ELISA approach based on coiled-coil interactions. *J. Immunol. Methods* **2010**, *362*, 161−167.
(27) Tripet, B.; Yu, L.; Bautista, D. L.; Wong, W. Y.; Irvin, R. T.; Hodges, R. S. Engineering a de novo-designed coiled-coil heterodimerization domain off the rapid detection, purification and characterization of recombinantly expressed peptides and proteins. *Protein Eng.* **1996**, *9*, 1029−1042.
(28) Boucher, C.; Liberelle, B.; Jolicoeur, M.; Durocher, Y.; De Crescenzo, G. Epidermal growth factor tethered through coiled-coil interactions induces cell surface receptor phosphorylation. *Bioconjugate Chem.* **2009**, *20*, 1569−1577.
(29) Oliverio, R.; Patenaude, V.; Liberelle, B.; Virgilio, N.; Banquy, X.; De Crescenzo, G. Macroporous dextran hydrogels for controlled growth factor capture and delivery using coiled-coil interactions. *Acta Biomater.* **2022**, *153*, 190−203.
(30) Boucher, C.; St-Laurent, G.; Loignon, M.; Jolicoeur, M.; De Crescenzo, G.; Durocher, Y. The Bioactivity and Receptor Affinity of Recombinant Tagged EGF Designed for Tissue Engineering Applications Is Defined by the Nature and Position of the Tags. *Tissue Eng., Part A* **2008**, *14*, 2069−2077.
(31) Noel, S.; Fortier, C.; Murschel, F.; Belzil, A.; Gaudet, G.; Jolicoeur, M.; De Crescenzo, G. Co-immobilization of adhesive peptides and VEGF within a dextran-based coating for vascular applications. *Acta Biomater.* **2016**, *37*, 69−82.
(32) Gerling-Driessen, U. I. M.; Mujkic-Ninnemann, N.; Ponader, D.; Schöne, D.; Hartmann, L.; Koksch, B.; Gerling-Driessen, U. I. M.; Schöne, D.; Koksch, B.; Ponader, D.; et al. Exploiting Oligo(amido amine) Backbones for the Multivalent Presentation of Coiled-Coil Peptides. *Biomacromolecules* **2015**, *16*, 2394−2402.
(33) Riahi, N.; Cappadocia, L.; Henry, O.; Omichinski, J.; De Crescenzo, G. Soluble expression, purification and functional characterization of a coil peptide composed of a positively charged and hydrophobic motif. *Amino Acids* **2016**, *48*, 567−577.
(34) Tallec, G.; Loh, C.; Liberelle, B.; Garcia-Ac, A.; Duy, S. V.; Sauvé, S.; Banquy, X.; Murschel, F.; De Crescenzo, G. Adequate Reducing Conditions Enable Conjugation of Oxidized Peptides to Polymers by One-Pot Thiol Click Chemistry. *Bioconjugate Chem.* **2018**, *29*, 3866−3876.
(35) Sehgal, D.; Vijay, I. K. A method for the high efficiency of water-soluble carbodiimide-mediated amidation. *Anal. Biochem.* **1994**, *218*, 87−91.
(36) Navratilova, I.; Papalia, G. A.; Rich, R. L.; Bedinger, D.; Brophy, S.; Condon, B.; Deng, T.; Emerick, A. W.; Guan, H. W.; Hayden, T.; et al. Thermodynamic benchmark study using Biacore technology. *Anal. Biochem.* **2007**, *364*, 67−77.
(37) Murschel, F.; Liberelle, B.; St-Laurent, G.; Jolicoeur, M.; Durocher, Y.; De Crescenzo, G. Coiled-coil-mediated grafting of bioactive vascular endothelial growth factor. *Acta Biomater.* **2013**, *9*, 6806−6813.
(38) Murschel, F.; Fortier, C.; Jolicoeur, M.; Hodges, R. S.; De Crescenzo, G. Two Complementary Approaches for the Controlled Release of Biomolecules Immobilized via Coiled-Coil Interactions: Peptide Core Mutations and Multivalent Presentation. *Biomacromolecules* **2017**, *18*, 965−975.
(39) De Crescenzo, G.; Boucher, C.; Durocher, Y.; Jolicoeur, M. Kinetic Characterization by Surface Plasmon Resonance-Based Biosensors: Principle and Emerging Trends. *Cell. Mol. Bioeng.* **2008**, *1*, 204−215.
(40) Homola, J. Present and future of surface plasmon resonance biosensors. *Anal. Bioanal. Chem.* **2003**, *377*, 528−539.
(41) Ellman, G. L. Tissue sulfhydryl groups. *Arch. Biochem. Biophys.* **1959**, *82*, 70−77.
(42) Myszka, D. G. Improving biosensor analysis. *J. Mol. Recognit.* **1999**, *12*, 279−284.
(43) Karlsson, R.; Pol, E.; Frostell, Å. Comparison of surface plasmon resonance binding curves for characterization of protein interactions and analysis of screening data. *Anal. Biochem.* **2016**, *502*, 53−63.
(44) Shrestha, B. R.; Liberelle, B.; Murschel, F.; Purisima, E. O.; Sulea, T.; De Crescenzo, G.; Banquy, X. Binding mechanism of a de novo coiled coil complex elucidated from surface forces measurements. *J. Colloid Interface Sci.* **2021**, *581*, 218−225.
(45) Hunter, T.; Cooper, J. A. Epidermal growth factor induces rapid tyrosine phosphorylation of proteins in A431 human tumor cells. *Cell* **1981**, *24*, 741−752.
(46) Davis, T. M.; Wilson, W. D. Determination of the refractive index increments of small molecules for correction of surface plasmon resonance data. *Anal. Biochem.* **2000**, *284*, 348−353.
(47) Ozcan, F.; Klein, P.; Lemmon, M. A.; Lax, I.; Schlessinger, J. On the nature of low- and high-affinity EGF receptors on living cells. *Proc. Natl. Acad. Sci. U.S.A.* **2006**, *103*, 5735−5740.
(48) Murschel, F.; Zaimi, A.; Noel, S.; Jolicoeur, M.; De Crescenzo, G. Specific Adsorption via Peptide Tags: Oriented Grafting and Release of Growth Factors for Tissue Engineering. *Biomacromolecules* **2015**, *16*, 3445−3454.
(49) Cambay, F.; Forest-Nault, C.; Dumoulin, L.; Seguin, A.; Henry, O.; Durocher, Y.; De Crescenzo, G. Glycosylation of Fcγ receptors influences their interaction with various IgG1 glycoforms. *Mol. Immunol.* **2020**, *121*, 144−158.
(50) Forest-Nault, C.; Gaudreault, J.; Henry, O.; Durocher, Y.; De Crescenzo, G. On the Use of Surface Plasmon Resonance Biosensing to Understand IgG-FcγR Interactions. *Int. J. Mol. Sci.* **2021**, *22*, 6616.
(51) Lequoy, P.; Savoji, H.; Saoudi, B.; Bertrand-Grenier, A.; Wertheimer, M. R.; De Crescenzo, G.; Soulez, G.; Lerouge, S. In Vitro and Pilot In Vivo Evaluation of a Bioactive Coating for Stent Grafts Based on Chondroitin Sulfate and Epidermal Growth Factor. *J. Vasc. Interv. Radiol.* **2016**, *27*, 753−760.e3.

https://doi.org/10.1021/acsomega.3c02172
ACS Omega 2023, 8, 28301−28313

(52) Fortier, C.; De Crescenzo, G.; Durocher, Y. A versatile coiled-coil tethering system for the oriented display of ligands on nanocarriers for targeted gene delivery. *Biomaterials* **2013**, *34*, 1344−1353.
(53) Dånmark, S.; Aronsson, C.; Aili, D. Tailoring Supramolecular Peptide−Poly(ethylene glycol) Hydrogels by Coiled Coil Self-Assembly and Self-Sorting. *Biomacromolecules* **2016**, *17*, 2260−2267.

Recommended by ACS

Folding-Assisted Peptide Disulfide Formation and Dimerization

Clara G. Victorio and Nicholas Sawyer

JUNE 30, 2023
ACS CHEMICAL BIOLOGY
READ

Manipulating Cation−π Interactions of Reader Proteins in Living Cells with Genetic Code Expansion

Hongxia Zhao, Shixian Lin, *et al.*

JULY 11, 2023
JOURNAL OF THE AMERICAN CHEMICAL SOCIETY
READ

Design and Evolution of Enhanced Peptide–Peptide Ligation for Modular Transglutaminase Assembly

Anthony H. Keeble, Mark Howarth, *et al.*

JUNE 08, 2023
BIOCONJUGATE CHEMISTRY
READ

Coiled-Coil-Based Biofunctionalization of 100 nm Gold Nanoparticles with the Trastuzumab Antibody for the Detection of HER2-Positive Cancer Cells

Médéric Dégardin, Gregory De Crescenzo, *et al.*

AUGUST 15, 2023
LANGMUIR
READ

Get More Suggestions >

https://doi.org/10.1021/acsomega.3c02172
ACS Omega 2023, 8, 28301−28313